

Signal transport in and conductance of correlated nanostructures

Peter Schmitteckert

DFG Center for Functional Nanostructures, Karlsruhe Institute of Technology, 76128 Karlsruhe, Germany and
Institute of Nanotechnology, Karlsruhe Institute of Technology, 76344 Eggenstein-Leopoldshafen, Germany

Here we report on our project concerning the application of time dependent DMRG to strongly correlated systems. We show that a previously reported simulation of the spin charge separation in a one-dimensional Hubbard system exceeds a relative error of 100% in the spin sector. In the second part we discuss the application of the Kubo formula to obtain linear conductance for the interacting resonant level model.

Transport properties of strongly interacting quantum systems are a major challenge in today's condensed matter theory. While much is known for transport properties of non-interacting electrons, based on the Landauer Büttiker formalism, the non equilibrium properties of interacting fermions are an open problem. Due to the vast improvements in experimental techniques there is an increasing theoretical interest in one-dimensional quantum systems. Since in low dimension the screening of electrons is reduced the effective interaction gets increased and can drive the electron systems into new phases beyond the standard description of a Fermi liquid, e.g. into a Luttinger liquid.

Formally the conductance of a quantum device attached to leads is given by the Meir Wingreen formula. Besides the special case of proportional coupling, the Meir Wingreen can only be treated within perturbative approaches.

The density matrix renormalization group method²⁻⁴ is a well established method to treat onedimensional interacting quantum systems. In this project we apply the real time evolution within the density matrix renormalization group method (RT-DMRG) to simulate the signal transport in onedimensional, interacting quantum systems, and the conductance of interacting nanostructures attached to onedimensional, non-interacting leads. In addition we calculate the conductance from the current-current and current-density correlations functions as a comparison to the real time evolution scheme and as a tool as itself, as it allows for a higher energy resolution as compared to the real time approach.

In this project we developed a DMRG code applying Posix threads to parallelize the code which is described in detail in⁸. While the DMRG is an approximative scheme, it has a systematic parameter, namely the number of states kept per block, to increase the accuracy of the calculation. In section I we show that this code allows us to perform systematic studies of the accuracy of transport problems. The major problem that arose during our previous work⁵⁻⁸ lies in the large resources needed to perform the actual simulation. In section II we show that we have now reformulated the Kubo approach which allows us to obtain a much higher energy resolution and that we could get rid of numerical instabilities.

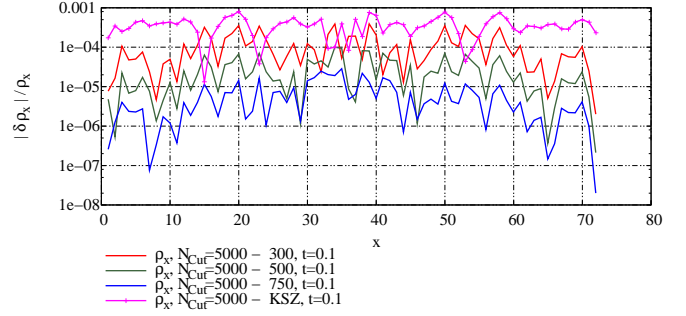


FIG. 1: Comparison of the electron density $n(x)$ of KSZ and our calculations keeping 300, 500, and 750 states per block, $M = 72$ sites, $N_\uparrow = N_\downarrow = 28$ with a reference calculation keeping 5000 states per block at time step $t=0.1$.

I. SPIN CHARGE SEPARATION

The spin charge separation of a single electron excitation is a prominent example of interaction effects in onedimensional electron systems. The first numerical observation was performed with an exact diagonalization approach by Karen Hallberg et al.⁹ for a 16 site system. Kollath et al.¹⁰ reported a simulation on a 72 site system with hard wall boundary conditions and 56 electrons. In⁸ we showed that with our code it is possible to study spin charge separation within the frame work of RT-DMRG for a $2/3$ filled 33 site Hubbard chain with periodic boundary conditions (PBC). The advantage of PBC lies in the absence of Friedel oscillations from the boundary. It turned out that for accurate results we should at least use of the order of 2000 states per block, which is considerably more than applied in¹⁰.

Here we compare the results of Kollath et al.¹⁰ (KSZ) who employed an adaptive RT-DMRG scheme combined with a Trotter decomposition^{11,12} with results obtained from our code⁸ where we combine the adaptive scheme with a Krylov based matrix exponential⁷. The system is a 72 site Hubbard model with an on site interaction of $U = 4.0$. The perturbation was created by applying a Gaussian perturbation to the potential of the up-electrons in the same way as described in⁷.

In Fig. 1 (2) we plot the relative accuracy of the electron density $n(x)$ (and its spin component $S^z(x) = (n_\uparrow(x) - n_\downarrow(x))/2$) at time step $t = 0.1$. It shows that

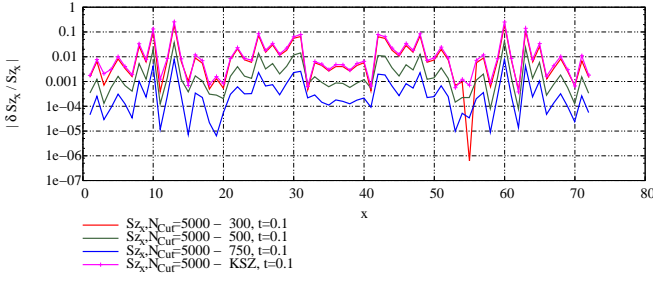


FIG. 2: Comparison of $S^z(x)$ of KSZ and our calculations keeping 300, 500, and 750 states per block with a reference calculation keeping 5000 states per block at time step $t=0.1$.

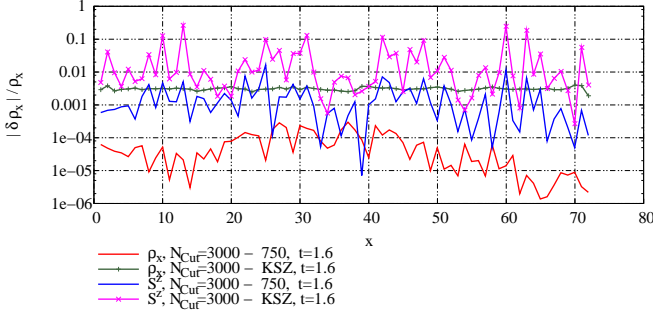


FIG. 3: Comparison of the density $n(x)$ and $S^z(x)$ of KSZ and our calculations keeping 750 states per block with a reference calculation keeping 3000 states per block at time step $t=1.6$ after an initial run keeping 5000 states up to $t = 0.1$.

KSZ and a 300 state calculation already have a relative accuracy which exceeds 10^{-3} for the electron density, while for the spin component one has to go up to 750 to achieve an accuracy of the order of 10^{-3} . The relative accuracy for the spin component is much harder as it can get close to zero.

After performing an initial calculation keeping 5000 states per block up to time $t = 0.1$, we continued the time evolution with 3000 states per block up to $t = 12$. In Fig. 3 we compare our results with KSZ and a calculation keeping 750 states per block. It shows that keeping 750 states per block we can still obtain an accuracy below 1% for the density and the spin component, while KSZ achieve an accuracy of 1% only for the density, while the spin component goes above an error of 10%.

Finally we compare the results of KSZ with our reference calculation keeping 3000 states per block at time step $t = 11.6$. While KSZ are able to achieve an accuracy of 1% for the absolute numbers, the spin component shows a relative deviation larger than a few hundred percent. While we have to be careful whether our results can be trusted at $t = 11.6$ to serve as an accuracy benchmark, the calculation should be much more accurate than the one performed by KSZ. In summary we have shown that one has to be very careful when employing the real time extensions to the DMRG. However, DMRG allows for a systematic check of the results which

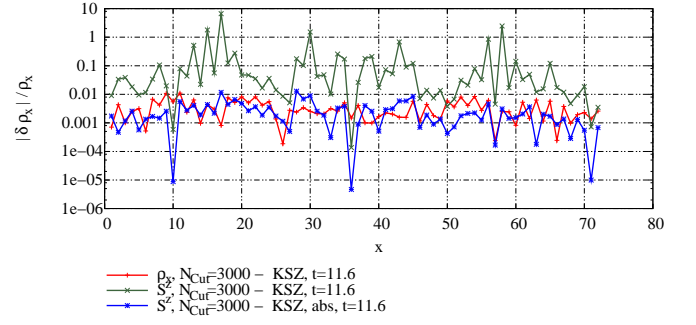


FIG. 4: Comparison of the density $n(x)$ and $S^z(x)$ of KSZ with a reference calculation keeping 3000 states per block at time step $t=11.6$ after an initial run keeping 5000 states up to $t = 0.1$. For the $S^z(x)$ component we plot the relative and the absolute difference.

is a very important property in a field where no other benchmarks are available.

II. LINEAR RESPONSE WITH MOMENTUM LEADS

Linear response calculations within DMRG⁶ provide a method to calculate the conductance of a nanostructure attached to leads. As it is based on the exact Kubo formula for the linear conductance $g \equiv \frac{e^2}{h} \langle \hat{J} \rangle / V_{SD}$ it is valid for arbitrary interaction. In the DC limit the conductance can be expressed in terms of two different correlators,

$$g_{J_N} = -\frac{e^2}{h} \langle \psi_0 | \hat{J}_{n_j} \frac{4\pi i \eta}{(\hat{H}_0 - E_0)^2 + \eta^2} \hat{N} | \psi_0 \rangle, \quad (1)$$

$$g_{JJ} = \frac{e^2}{h} \langle \psi_0 | \hat{J}_{n_1} \frac{8\pi \eta (\hat{H}_0 - E_0)}{[(\hat{H}_0 - E_0)^2 + \eta^2]^2} \hat{J}_{n_2} | \psi_0 \rangle, \quad (2)$$

where the positions n_j are in principle arbitrary. However, the positions n_1 and n_2 should be placed close to the nanostructure to minimize finite size effects. Bohr, Wölfle and Schmitteckert⁶ had to introduce exponentially reduced hopping terms close to the boundary of the leads which had been described in real space to minimize finite size effects, which in return leads to ill-conditioned linear systems. In order to solve these equations, they had to employ scaling sweeps to switch on the damping in the leads gradually. While the method proved to be a valuable tool it turned out that it is getting too expensive to study more interesting systems.

Recently we have developed a new scheme¹³ based on leads described in momentum space to overcome the difficulties we encountered in⁶, for details see also⁸. While it is generally accepted that DMRG does not work well in a momentum space description due to the large amount of couplings intersecting the artificial cut of the system into two parts within DMRG, our transport calculation are performed with non interacting leads. Therefore the

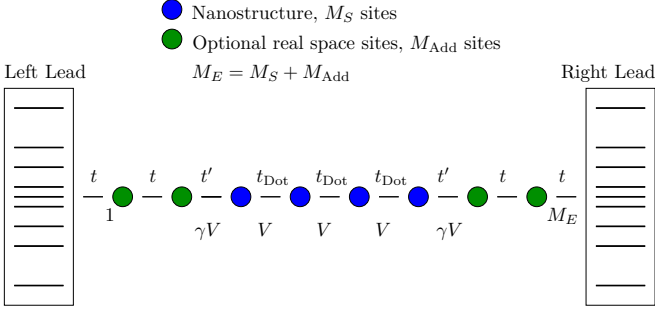


FIG. 5: Schematics of the leads coupled to the nanostructure.

number of links intersecting the DMRG splitting of the system is vastly reduced.

In order to be able to describe processes on different energy scales we first couple our nanostructure to a few sites in real space to capture local, i.e. high energy, physics. Then we employ a logarithmic discretization of the momentum leads to cover a large energy range and finally we use a linear discretization of the low energy scale in order to describe low energy transport properties accurately. We would like to note that these additional sites on a linear discretization close to the Fermi edge are beyond a NRG like description. While they are not needed for a qualitative description, they enable us to get very accurate results even close to the resonant tunneling regime. The reason for that lies in the nature of transport properties, where the η in the correlation function plays a much more important role than for equilibrium properties. It does not only provide a smoothing of the poles, it has to create excitations which then can actually lead to transport.

The models considered in this work are the interacting resonant level model (IRLM) and the natural extension of this model to linear chains, defined by the Hamiltonians

$$H_{RS} = \sum_{j \in S} \mu_g \hat{c}_j^\dagger \hat{c}_j - \sum_{j,j-1 \in S_E} (t_j \hat{c}_j^\dagger \hat{c}_{j-1} + \text{h.c.}) + \sum_{j,j-1 \in S_E} V_j \left(\hat{n}_j - \frac{1}{2} \right) \left(\hat{n}_{j-1} - \frac{1}{2} \right), \quad (3)$$

$$H_{MS} = \sum_{k \in L,R} \epsilon_k \hat{c}_k^\dagger \hat{c}_k, \quad (4)$$

$$H_T = -t_k \left(\sum_{k \in L} \hat{c}_k^\dagger \hat{c}_1 + \sum_{k \in R} \hat{c}_k^\dagger \hat{c}_{M_E} \right) + \text{h.c.}, \quad (5)$$

where \hat{c}_ℓ^\dagger and \hat{c}_ℓ (\hat{c}_k^\dagger and \hat{c}_k) are the spinless fermionic creation and annihilation operators at site ℓ (momentum k), $\hat{n}_\ell = \hat{c}_\ell^\dagger \hat{c}_\ell$. H_{RS} , H_{MS} , and H_T denote real space, momentum space, and tunneling between real- and momentum space Hamiltonians respectively. The symbols S and S_E denote the nanostructure and the extended nanostructure (the full real space chain) respectively. The indices 1 and M_E denote the first and last site in S_E . The general setup and the specific values of the hopping matrix elements t_j and the interactions V_j are indicated in

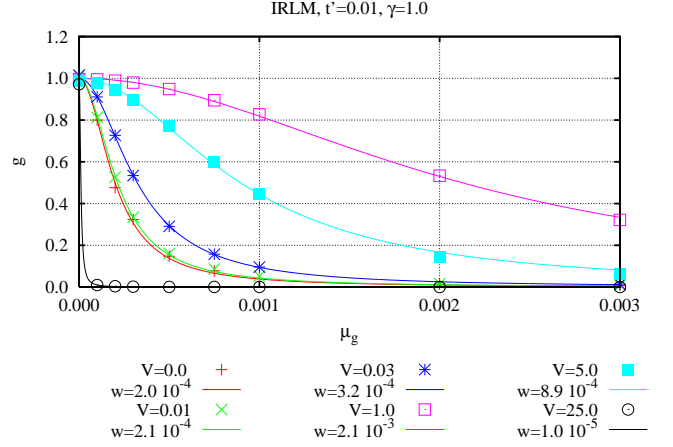


FIG. 6: Linear conductance versus gate potential for the interacting resonant level model for $t' = 0.01$ and a interaction on the contacts ranging from zero to 25. To each set of DMRG data a Lorentzian of half width $2w$ has been added as a guide to the eye. The leads are described with a cosine band between ± 2 such that the Fermi velocity is $v_F = 2$. In contrast to intradot interaction the interaction on the contacts enhances the conductance and shows a non monotonic behavior versus contact interaction.

Fig. 5, and note specifically the interactions on the contact links, γV . The momentum dependent coupling t_k is chosen to represent an infinite onedimensional tight-binding chain if a cosine band $\epsilon_k = -2t \cos(k)$ is chosen. All energies are measured in units of $t = 1$.

In fig. 6 we show the linear conductance versus gate potential for a contact hopping of $t' = 0.01$ and interaction on the contacts ranging from zero to 25. The calculations have been performed with 130 sites in total, $M_E = 10$ real space sites, and 120 momentum space sites. Due to the symmetry of the band we used a discretization that is symmetric around $\epsilon_F = 0$, and applied an identical discretization scheme to both leads. To represent the ‘large’ energy span in the band we used 20 logarithmically scaled sites, and thereafter used 10 linearly spaced sites to represent the low energy scale correctly. In the DMRG calculations presented we used at least 1300 states per block and 10 finite lattice sweeps.

The data demonstrates a strong increase of the resonance width due to interaction up to a factor of ten. The increase of the resonance width due to interaction on the contact is in contrast to the reduction of conductance due to interaction on nanostructures, see⁶. Once interaction is larger than the Fermi velocity the resonance width gets strongly reduced. The results also shows that we can now resolve resonance width of the order 10^{-5} . We would like to note that this scheme is not restricted to single impurity models and that it also works for extended nanostructures.

The implementation of this new scheme was only finished recently and we are currently extending it to include the spin degree of freedom. In detail we study the

single impurity Anderson model attached to polarized, ferromagnetic leads.

III. FURTHER PROJECTS

The code developed within this project has also been used in¹⁴ to study quantum phase transition with entanglement entropy and in¹⁵ to study onedimensional fermions in a harmonic trap with an attractive on site interaction. In¹⁶ we used the DMRG to extract the exact corresponding functionals of a lattice Density Functional Theory and compared the conductance calculations within DMRG and DFT.

IV. POST-PUBLICATION NOTE

In the code applied within this report, some off-diagonal blocks were missing in the construction of the

reduced density matrix for the time-dependent simulation. In return the selected basis is sub-optimal. We checked with a corrected code version, that the induced error is indeed small, especially for the 5000 states. The content of the report is not affected. The results of our td-DMRG variant could just have been a little bit better.

Acknowledgments

We would like to thank Corinna Kollath for interesting discussions and for providing us with the raw data of¹⁰. This work profited from the parallelization performed within the project 710 of the Landesstiftung Baden-Württemberg. The reformulation of the momentum leads was performed together with Dan Bohr within the HPC-EUROPA project RII3-CT-2003-506079. Most of the calculations have been performed at the XC1 and XC2 of the SSC Karlsruhe under the grant number RT-DMRG.

¹ Y. Meir and N. S. Wingreen, Phys. Rev. Lett. **68**, 2512 (1992).

² S. R. White, Phys. Rev. Lett. **69**, 2863 (1992).

³ S. R. White, Phys. Rev. B **48**, 10345 (1993).

⁴ Density Matrix Renormalization – A New Numerical Method in Physics, edited by I. Peschel, X. Wang, M. Kaulke, and K. Hallberg (Springer, Berlin, 1999); Reinhard M. Noack and Salvatore R. Manmana, Diagonalization- and Numerical Renormalization-Group-Based Methods for Interacting Quantum Systems, AIP Conf. Proc. 789, 93-163 (2005).

⁵ Günter Schneider and Peter Schmitteckert: *Conductance in strongly correlated 1D systems: Real-Time Dynamics in DMRG*, condmat-0601389.

⁶ Dan Bohr, Peter Schmitteckert, Peter Wölfle: *DMRG evaluation of the Kubo formula – Conductance of strongly interacting quantum systems*, Europhys. Lett., **73** (2), 246 (2006).

⁷ Peter Schmitteckert: *Nonequilibrium electron transport using the density matrix renormalization group*, Phys. Rev. B **70**, 121302 (2004).

⁸ Günter Schneider and Peter Schmitteckert: *Signal transport and finite bias conductance in and through correlated nanostructures* p. 113 -126 in W.E. Nagel, W. Jäger, M. Resch (Eds.), “High Performance computing in Science

and Engineering '06”, Springer Verlag Berlin Heidelberg 2007, ISBN 978-3-540-36165-7.

⁹ E. A. Jagla, K. Hallberg, C. A. Balseiro, Phys. Rev. B **47**, 5849 (1993).

¹⁰ C. Kollath, U. Schollwoeck, W. Zwerger, Phys. Rev. Lett. **95**, 176401 (2005).

¹¹ S. R. White and A. E. Feiguin, Phys. Rev. Lett. **93**, 076401 (2004).

¹² A. J. Daley, C. Kollath, U. Schollwöck, and G. Vidal, J. Stat. Mech.: Theor. Exp. P04005 (2004).

¹³ Dan Bohr and Peter Schmitteckert: *Strong enhancement of transport by interaction on contact links*, Phys. Rev. B **75** 241103(R) (2007).

¹⁴ Rafael A. Molina and Peter Schmitteckert, *Numerical estimation of critical parameters using the bond entropy*, Phys. Rev. B **75**, 235104 (2007).

¹⁵ Rafael A. Molina, Jorge Dukelsky, and Peter Schmitteckert, *Commensurability effects for fermionic atoms trapped in 1D optical lattices*, arXiv:0707.3209, Phys. Rev. Lett. **99**, 080404 (2007).

¹⁶ Peter Schmitteckert and Ferdinand Evers, *Exact ground state density functional theory for impurity models coupled to external reservoirs and transport calculations*, arXiv:0706.4253, Phys. Rev. Lett. **100**, 086401 (2008).